Title

Derivation of EEG information from rates of change in order parameter and free energy dissipation.

Journal

Conference proceedings : ... Annual International Conference of the IEEE Engineering in Medicine and Biology Society. IEEE Engineering in Medicine and Biology Society. Conference, 6(1)

ISSN

1557-170X

Author

Freeman, Walter J, III

Publication Date

2004-09-01

Proceedings of the 26th Annual International Conference of the IEEE EMBS
San Francisco, CA, USA • September 1-5, 2004

Derivation of EEG information from rates of change in order parameter and free energy dissipation

Walter J Freeman
Department of Molecular and Cell Biology, University of California at Berkeley CA 94720-3200, USA

Abstract— **EEG patterns correlated with conditioned stimuli were sought in amplitude modulation of synchronous beta-gamma oscillations (12-80 Hz). EEG signals were recorded from high-density 8x8 (5.6x5.6 mm) arrays fixed on the surfaces of primary sensory areas in rabbits trained to discriminate visual, auditory, or tactile conditioned stimuli. EEG preprocessing was by (i) band pass filtering to extract the beta-gamma range (deleting theta-alpha); (ii) low-pass spatial filtering (not high-pass Laplacians used for localization), (iii) spatial averaging (not time averaging used for evoked potentials); (iv) close spacing of electrodes for simultaneous recording in each area (not sampling single signals from several areas); (v) calculating variances among patterns in 64-space derived from the 8x8 arrays (not by fitting equivalent dipoles). These methodological differences were essential to reveal discontinuities in cortical activity: "state transitions". Each transition began with an abrupt phase re-setting, followed sequentially by resynchronization, stabilization of a spatial pattern of amplitude, and dramatic increase in global pattern amplitude. State transitions recurred at irregular intervals in the theta range. An estimate of perceptual information in the beta-gamma EEG disclosed 2 to 3 patterns with high information content in each trial that began with a state transition, lasted ~0.1 s, and recurred at theta rates.**

Keywords—**Electroencephalogram EEG, neural imaging, perception, spatial pattern analysis, state transition, synchrony**

I. Introduction

Synchrony of firing of widely distributed neurons in large numbers is necessary for emergence of spatial structure in cortical activity by reorganization of unpatterned background activity. The dendritic currents regulate the firing. The same currents are largely responsible for local field potentials and EEG. The firing is grouped in time by oscillations in dendritic current in the beta (12-30 Hz) and gamma (30-80 Hz) ranges that arise from negative feedback among excitatory and inhibitory neurons [1, 2]. The synchrony among multiple EEG records has been evaluated by measuring the phase of the EEG record from each channel with respect to the phase of the spatial average EEG over all channels and calculating the standard deviation (SD_X) of the spatial distribution of phase values [3]. While conceptually simple, the use of phase has formidable obstacles, because EEG signals are aperiodic ("chaotic"). Two features of the EEG from high-density 2-D arrays offered an alternative approach. First, EEG signals from arrays up to 1 cm in width were highly correlated but with varying patterns of amplitude modulation. Second, the spatial patterns of phase modulation across the array showed epochs of low SD_X that were bracketed by brief episodes of high variance [4] showing that high synchrony was episodic.

In the present study EEG signals were temporally filtered in the beta or gamma range. The temporal standard deviation (SD_T) was got for the spatial average waveform in each epoch lasting T digitizing steps, where T was twice the wavelength at the peak frequency in the interval. The SD_T was divided by the average of the standard deviation of all 64 waveforms ($\underline{SD}_T$) in the epoch. If the EEG signals were completely synchronous, the ratio would be unity. To the extent that the EEG signals deviated from the average in amplitude, phase or frequency, they tended to cancel, so that the ratio decreased markedly as the signals approached independence. This method of estimating synchrony avoided measuring phase explicitly, so it was suitable for evaluating synchrony among multiple aperiodic "chaotic" signals.

II. Methodology

The 8x8 electrode spacing of 0.79 mm gave a spatial aperture 5.6x5.6 mm. Signals with analog pass band .1-100 Hz were amplified 10K, digitized at 500 Hz with 12-bit ADC, and stored in a 64x3,000 matrix for each 6-s trial [5]. Rabbits were trained in a classical conditioning paradigm with 20 trials using a reinforced conditioned stimulus (CS+) and 20 trials of an unreinforced CS- randomly alternated. The data consisted of 5 trials from each of 6 rabbits, 2 each with an 8x8 array on the visual, auditory or somatic cortices. The 64 EEG signals in each trial were preprocessed with MATLAB software by de-meaning to remove channel bias, normalizing to unit SD, spatial low pass filtering at 0.3 c/mm to attenuate channel noise, and temporal band pass filtering at 20-80 Hz to retain high beta and gamma activity.

III. Results

The EEGs, $v_j(t)$, j = 1,64, served to estimate the dendritic current of excitatory neurons in the forward limb of the cortical negative feedback loop and to give the "real part" of the analytic amplitude in Hilbert terminology [6, 7]. The Hilbert transform of $v_j(t)$ gave an estimate of the output, $v'_j(t)$, of the inhibitory neurons in the feedback limb of the negative feedback loop, which maintained an oscillation at the same frequency but with approximately a quarter cycle lag behind the output of the excitatory neurons [1, 2]. This "imaginary part" and its spatial ensemble average, $iv_j'(t)$, approximated the negative rate of change of $\underline{v}(t)$. At each digitizing step j (2 ms) the real part, $v_j(t)$ and imaginary part,

$iv_j'(t)$, determined a point in polar coordinates, which was the tip of a vector, $V_j(t)$, extending to that point from the origin of the complex plane at $v_j(t) = 0$ and $i\,v_j'(t) = 0$.

$$V_j(t) = v_j(t) + iv_j'(t). \quad (1)$$

Successive pairs of values specified the trajectory of the tip of the average vector, $\underline{V}(t)$, as it rotated counterclockwise about the origin of the complex plane with time. The analytic amplitude for each channel, $A_j(t)$, was the length of the vector, which was given by the square root of the sums of squares of the real and the imaginary parts for each channel. The average was denoted $\underline{A}(t)$.

$$A_j(t) = [v_j^2(t) + v_j'^2(t)]^{0.5} \quad (2)$$

The waveform of the average analytic amplitude, $\underline{A}(t)$, over the 64 channels was always ≥ 0. The analytic phase, $P_j(t)$, for the j-th channel was given by the arctangent of the ratio of the imaginary part to the real part .

$$P_j(t) = \text{atan}\,[v_j'(t)\,/v_j(t)] \quad (3)$$

The analytic phase was unwrapped by adding π radians at each break point to get $p_i(t)$. **Fig. 1** shows a raster plot of the 64 sequential phase differences, $\Delta p_j(t)$. Phase slip was revealed by upward or downward deviations from the mean differences, $\Delta \underline{p_j}(t)$. These jumps occurred synchronously across the entire 8x8 array, here plotted in a compressed display of $\Delta p_j(t)$ in the order of channel number. The coordination of the jumps was measured by the spatial standard deviation, $SD_X(t)$, of $\Delta \underline{p_j}(t)$ (**Fig. 2, A**, dark curve). Superimposing the spatial ensemble average of $\underline{A}(t)$ (grey curve) showed that maximal $SD_X(t)$ tended to occur most often when analytic amplitude fell to low values.

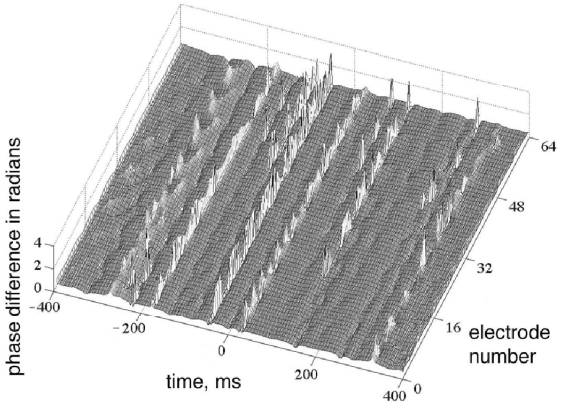

Fig. 1. The raster plot shows the successive differences of the unwrapped analytic phase, $\Delta p_j(t)$, changing with time (left abscissa) and channel (right abscissa). The 8 columns of 8 rows are aligned to show the near-coincidence of the sudden jumps and dips of phase slip given by fast-forward and backward rotation of the vector defined by equation (1). When jumps or dips were aligned with the right abscissa, they showed nearly zero lags among them. Deviation from the direction of the right abscissa (as most clearly at about -250 ms) showed a phase gradient across the array that corresponded to the delays imposed by conduction velocities of cortical running axons parallel to the pia. From [2].

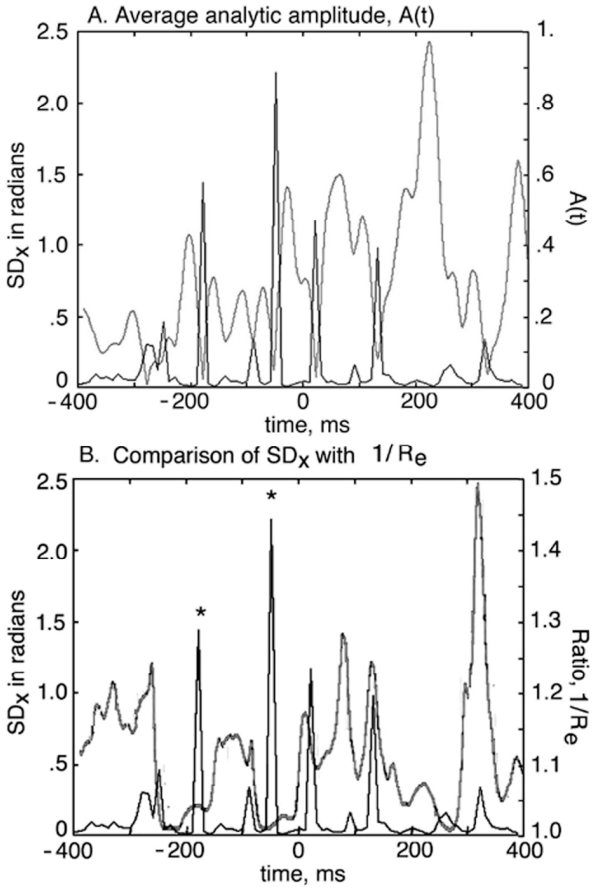

Fig 2. The spatial SD of phase differences across the array, $SD_X(t)$, (dark curve) was adopted as a reference to be used to compare other methods of indexing the degree of synchrony and other parameters. A. $SD_X(t)$ *vs.* analytic amplitude, $\underline{A}(t)$. B. $SD_X(t)$ *vs.* $1/R_e(t)$. The * show when $\underline{A}(t)$ fell to low values during episodes of maintained high synchrony. From [2].

The Hilbert transform was applied to the 64 signals on each trial from 37-40 6-s trials performed by each of 6 rabbits. The peak frequency of the filtered data was calculated from the FFT of the spatial ensemble average of the 64 $A_j(t)$. A sliding window of duration T = 2.0x the wavelength of the peak frequency of the FFT was stepped along the $A_j(t)$ at the digitizing interval. The window length, T, specified the "window order" in bins, w=T/2. The SD of $A^2_{j,,T}(t)$ in the window was computed for each channel to get the mean of the 64 $SD_{i,T}(t)$ across channels, $\underline{SD}_T$.

$$\underline{SD}_T(t) = 1/64\ \Sigma\ SD_{j,T}(t),\ j = 1, \ldots, 64, \quad (6)$$

The spatial ensemble average, $\underline{A}_T(t)$, of the 64 time series of $A_j(t)$ in the window was computed along with its SD_T. Their ratio was designated R_e. Its value was plotted as $1/R_e$ with the midpoint of the window at time t.

$$R_e(t) = SD_T \text{ of mean } \underline{A}(t) \,/\, \text{mean } \underline{SD}_T \quad (7)$$

The range of R_e was 1 for perfect synchrony to $1/T^{.5}$ for complete independence. In order to compare the time relations of R_e to the other measure of synchrony, SD_X, the ratio was inverted, $1/R_e$ (**Fig. 2, B**), A. Low values (grey

curve) demarcated time periods with high synchrony; high values showed periods of desynchronization.

Each spatial pattern of analytic amplitude squared, $A^2_j(t)$, of the 64 EEGs at each point in time specified a point in 64-space as the tip of a vector extending from the origin. The length of the vector, $\underline{A}^2(t)$, representing the global amplitude of each pattern gave the Euclidean distance to the origin. The 64 $A^2_j(t)$ in each frame were normalized to z-scores. The normalized spatial pattern gave a 64x1 column vector denoted in boldface as $\mathbf{A^2}(t)$. The increment of change in normalized spatial pattern, $\Delta\mathbf{A}^2(t)$, with each step Δt was given by the Euclidean distance, $D_e(t)$, between successive points in 64-space. An example of the time series is shown by the curve in **Fig. 3,** where it is compared with $1/R_e$ in (**A**) and with $\underline{A}(t)$ in **(B).** Low values of D_e indicated epochs of relative spatial pattern stability; high values of D_e revealed the time periods when spatial patterns were changing rapidly and could be regarded as unstable.

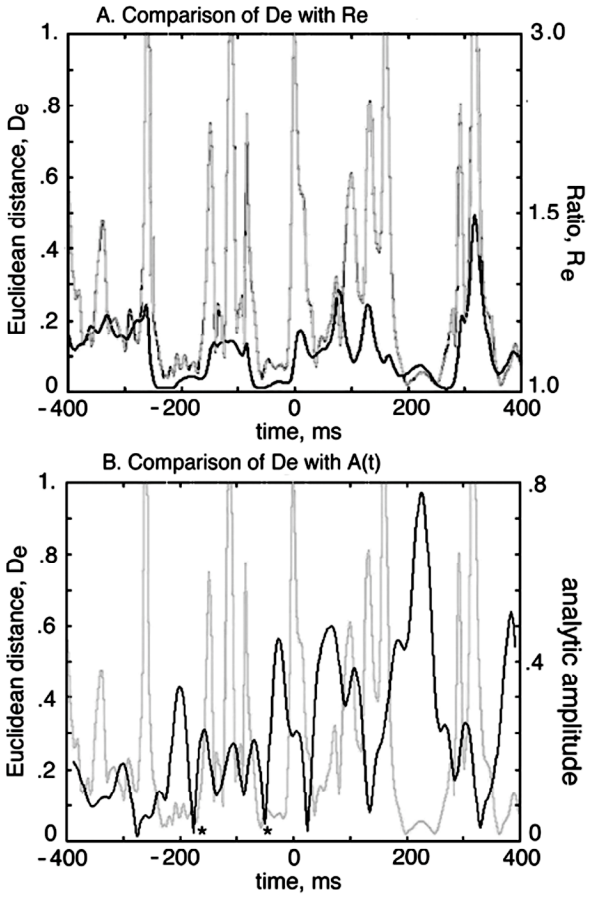

Fig. 3. A. $D_e(t)$ *vs.* $R_e(t)$. B. $D_e(t)$ *vs.* $\underline{A}(t)$. From [2].

IV. Discussion

The square of the amplitude of the normalized beta-gamma EEG (the real part, v(t), in equation (1)) provided an index of the power, $i^2(t)r$, used by the excitatory population to drive dendritic current, i(t), across the fixed extracellular tissue resistance, r. The square of the neocortical current i(t) was proportional to the power used by excitatory pyramidal cells (the real part in equation (1)). The curve calculated with the Hilbert transform (the imaginary part in equation (1)) approximated the negative of the temporal derivative of the EEG [6]. It also approximated the time course of activity of the inhibitory neuronal population that provided the feedback limb of the negative feedback loop by which the beta-gamma oscillations were generated [1]. The square of the imaginary part gave an index of the power used by the inhibitory population. The sum of squares of the real and imaginary parts, A_j^2, when integrated over the window used to measure the SD_X of A_j^2, gave an index of the free energy dissipation rate, E(t). The spatiotemporal pattern of A_j^2 was integrated over appropriate time and space windows to get $\mathbf{A^2}(t)$, serving to estimate the rate of patterned free energy dissipation by excitatory and inhibitory populations in the EPSPs and IPSPs manifested in beta-gamma oscillations.

The state vector, $\mathbf{A^2}(t)$, in 64-space specified a point representing the spatial pattern of a wave packet in each window. The length of the vector, $\underline{A}^2(t)$, indexed the power or intensity of the pattern. The pattern manifested the order in a synchronized domain of cortex that was accessed by a state transition elicited by thalamic input acting as a "control parameter" [8]. An "order parameter" [9] was defined as the intensity of the intracortical synaptic interactions, k, by which action potentials were synchronized. The emergence of order was symmetry breaking, and it carried the neocortex far from the pseudoequilibrium of its self-organized stable state, so that the order parameter, k, could vary with time, which it could not do in a system maintained at equilibrium. As shown by Prigogine [10] and Haken [9] on approach of a system far from equilibrium to a critical state transition is manifested by slowing of rate of change in the order parameter, $\Delta k/\Delta t$, and by increased amplitude of oscillations in the output. These were the changes that were revealed by R_e, D_e, and $\underline{A}(t)$. Thus shortly after reinitialization R_e approached unity manifesting resynchronization, followed by spatial order emerging in an abrupt decrease in D_e with Δt that signified a decrease in the rate of change of the order parameter, D_e,

$$\Delta\mathbf{A}^2(t)/\Delta t \sim \Delta k/\Delta t \sim D_e(t). \quad (8)$$

Next, the power manifested in the analytic amplitude began to increase without further increase in synchrony, which signified an increase in the rate of conversion of chemical free energy, dE/dt, to electrical energy,

$$\Delta E/\Delta t \sim \underline{A}^2(t), \quad (9)$$

which was then dissipated as heat. Maximal order emerged when the rate of change in D_e went briefly to zero, and transmission was maximized as the rate of free energy mobilization rose. This condition was numerically indexed by H_e (**Fig. 4**) defined as the ratio of the two rates of change,

$$H_e = -\partial E/\partial k \sim \underline{A}^2/D_e. \quad (10)$$

Maximal values of H_e were found to occur in the 600 ms interval after the onset of conditioned stimuli that the subjects had been trained to discriminate (**Fig. 5**).

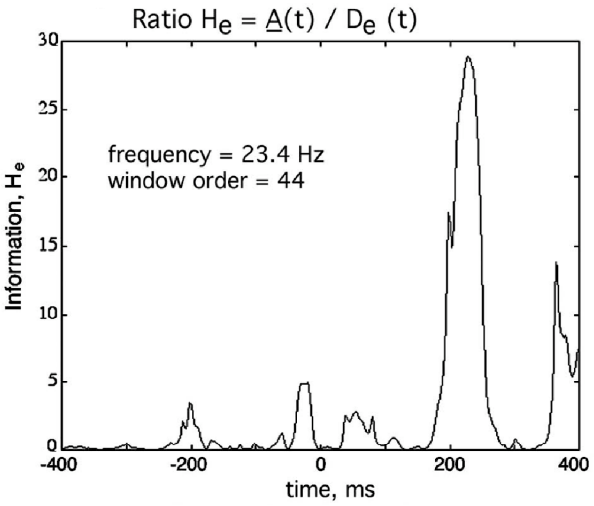

Fig. 4. Each state transition began with a discontinuity in phase (SD_X) that reinitialized cortical dynamics, leading to resynchronization (R_e), pattern selection and stabilization (D_e), and culminating in a dramatic increase in amplitude ($\underline{A}(t)$). Increase in the ratio H_e was greatest after stimulus arrival at t = 0. From [2].

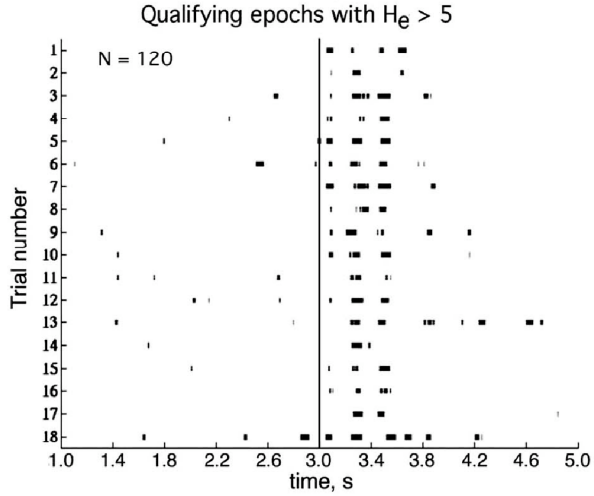

Fig. 5. $H_e(t)$ of visual cortical EEG was by equation (10) in the central 4 s each 6 s trials over a set of 18 trials. The distribution of log H_e was computed in 37 trials over a session, giving a nearly normal distribution. A threshold of 5 (log H_e = .7) served to locate the tail of high values that corresponded to high peaks in H_e after CS arrival at 3 s. High H_e epochs between onsets of CSs and conditioned responses with latency ranging 700-1200 ms (3.7-4.2 s) suggested that these epochs contained significant neural information that was correlated to goal-directed behavior. From [2].

V. Conclusion

This ratio (**Fig. 4**) is analogous in form to a definition of order by Haken [9, p. 181, equation 6.178], and to "pragmatic information" defined by Atmanspacher and Scheingraber [11] using the concept of "efficiency" [their equations 8-10] as a "fundamental extension of Shannonian information" [pp. 731-2]. Thus H_e is proposed as an index of the quantity of the information in wave packets that is displayed in sequences of their spatial patterns of amplitude modulation.

Acknowledgments

This study was supported by grant MH 06686 from the National Institute of Mental Health, grant NCC 2-1244 from the National Aeronautics and Space Administration, and grant EIA-0130352 from the National Science Foundation to Robert Kozma. Programming was by Brian C. Burke. Major contributions to surgery, training of animals, data acquisition, and data analysis by John Barrie, Gyöngyi Gaál, and Linda Rogers are gratefully acknowledged.

References

[1] Freeman WJ. Mass Action in the Nervous System. Academic Press, New York, 1975. Reprinted 2004: http://sulcus.berkeley.edu/MANSWWW/MANSWWW.html

[2] Freeman WJ. Origin, structure, and role of background EEG activity. Part 1. Analytic amplitude. Part 2. Analytic phase. Clin. Neurophysiol. In press.

[3] Freeman WJ, Burke BC, Holmes MD. Aperiodic phase re-setting in scalp EEG of beta-gamma oscillations by state transitions at alpha-theta rates. Hum. Brain Mapp. 19: 248-272, 2003.

[4] Freeman WJ, Rogers L.J. A neurobiological theory of meaning in perception. Part 5. Multicortical patterns of phase modulation in gamma EEG. Int. J. Bifurc. Chaos 13: 2867-2887, 2003.

[5] Barrie JM. Freeman WJ, Lenhart M. Modulation by discriminative training of spatial patterns of gamma EEG amplitude and phase in neocortex of rabbits. J. Neurophysiol. 76: 520-539, 1996.

[6] Pikovsky A, Rosenblum M, Kurths J. Synchronization — A Universal Concept in Non-linear Sciences. Cambridge UK: Cambridge U.P., 2001.

[7] Barlow JS. The Electroencephalogram: Its Patterns and Origins. Cambridge MA: MIT Press, 1993.

[8] Miller LM, Schreiner CE. Stimulus-based state control in the thalamocortical system. J. Neurosci. 20: 7011-7016, 2000.

[9] Haken, H. Synergetics: An Introduction. Berlin: Springer-Verlag, 1983.

[10] Prigogine I. From Being to Becoming: Time and Complexity in the Physical Sciences. WH Freeman, San Francisco, 1980.

[11] Atmanspacher H, Scheingraber H. Pragmatic information and dynamical instabilities in a multimode continuous-wave dye laser. Can. J. Phys. 68: 728-737, 1990.